Stable isotopes track biogeochemical processes under seasonal ice cover in a shallow, productive lake

Authors: Christopher H. Gammons, William Henne, Simon R. Poulson, Stephen R. Parker, Tyler B. Johnston, John E. Dore, & Eric S. Boyd

This is a postprint of an article that originally appeared in Biogeochemistry on August 2014. The final publication is available at Springer via http://dx.doi.org/10.1007/s10533-014-0005-z.

Gammons, Christopher H., William Henne, Simon R. Poulson, Stephen R. Parker, Tyler B. Johnston, John E. Dore, and Eric S. Boyd. "Stable isotopes track biogeochemical processes under seasonal ice cover in a shallow, productive lake." Biogeochemistry 120, no. 1-3 (2014): 359-379. http://dx.doi.org/10.1007/s10533-014-0005-z

Stable isotopes track biogeochemical processes under seasonal ice cover in a shallow, productive lake

Christopher H. Gammons & William Henne: Department of Geological Engineering, Montana Tech of The University of Montana, Butte, MT, USA
Simon R. Poulson: Department of Geological Sciences and Engineering, University of Nevada-Reno, Reno, NV, USA
Stephen R. Parker & Tyler B. Johnston: Department of Chemistry and Geochemistry, Montana Tech of The University of Montana, Butte, MT USA
John E. Dore: Department of Land Resources and Environmental Sciences, Montana State University, Bozeman, MT, USA
Eric S. Boyd: Department of Microbiology, Montana State Univerity, Bozeman, MT, USA

Abstract

Biogeochemical dynamics under seasonal ice cover were investigated in the shallow (<10 m) water column of highly productive Georgetown Lake, western Montana, USA. This high altitude (1,800 m) reservoir is well-mixed in summer, but becomes strongly stratified under ice cover (mid-November–mid-May). A rapid drop in dissolved oxygen (DO) concentration and rise in dissolved inorganic carbon (DIC) concentration was observed after the onset of ice, with a corresponding increase in δ^{18}O-DO and decrease in δ^{13}C-DIC, likely caused by respiration (R) of organic carbon. Photosynthesis/respiration ratios (P/R) estimated from simultaneous measurement of DO and δ^{18}O-DO were near unity prior to ice formation but then systematically decreased with time and depth in the lake under ice cover. P/R in the water column was higher at a shallower monitoring site compared to a deeper site near the dam outlet, which may have been important for over-winter survival of salmonids. By March, the bottom 3 m of the water column at both sites was anoxic, with the bottom 1 m being euxinic. Elevated concentrations of dissolved sulfide, ammonium, phosphate, Fe^{2+}, and Mn^{2+} in deep water suggest coupling of organic carbon degradation with reduction of a number of electron acceptors (e.g., Fe^{3+},NO_3^-, $SO^2_4^-$). The concentrations and δ^{34}S values of H_2S in the deep water and SO2i in the shallow water were similar, indicating near-complete reduction of sulfate in the euxinic zone. Late in the winter, an influx of isotopically heavy DIC was noted in the deep water coincident with a buildup of dissolved CH_4 to concentrations >1 mM. These trends are attributed to acetoclastic methanogenesis in the benthic sediments. This pool of dissolved CH_4 was likely released from the lake to the atmosphere during spring ice-off and lake turnover.

Electronic supplementary material The online version of this article (doi:10.1007/s10533-014-0005-z) contains supplementary material, which is available to authorized users.

Introduction

Seasonal ice cover is a characteristic feature of high-latitude and/or high-altitude lakes, and it exerts a strong control on energy and material transport to/from and within lake ecosystems. Nevertheless, there is presently a dearth of empirical information on winter biogeochemical processes occurring beneath the ice in such systems (Bertilsson et al. 2013). Given that climate warming is anticipated to continue to decrease the duration of seasonal lake ice cover (Weyhenmeyer et al. 2011; Dibike et al. 2012), it is important that we understand how lake ecosystems function in both ice-free and ice-covered seasons, and how the transitions between these states proceed. Of particular importance to the present study is the phenomenon of seasonal dissolved oxygen (DO) depletion in the hypolimnion of shallow, ice-covered lakes which, in some cases, can lead to winterkill of fish (Greenbank 1945; Mathias and Barica 1980; Babin and Prepas 1985). Depletions in DO are mainly caused by decomposition of plant matter grown in the preceding ice-free season that settles to the sediment interface. Aerobic respiration (R) may result in anoxic conditions in the winter hypolimnion of the lake, with a concomitant increase in reduced constituents, such as H_2S and ammonia produced through anaerobic respiratory pathways (Scidmore 1957). When electron acceptors such as O_2, NO_3^-, SO_4^{2-} are consumed, fermentation and methanogenesis may ensue, leading to accumulations of CH_4 in the water column (Bertilsson et al. 2013). Much of this CH_4 may be released to the atmosphere when the ice-covered season ends and vertical mixing takes place (Michmerhuizen et al. 1996). Several authors (e.g., Bastviken et al. 2003, 2004; Tranvik et al. 2009) have argued that emissions of CO_2 and CH_4 from temperate freshwater lakes have important consequences to the global carbon budget.

Whereas conventional water quality sampling is sufficient to define the existence of vertical chemical gradients in ice-covered lakes, an approach that combines chemical analysis and stable isotope analysis has the potential to yield more information on biogeochemical mechanisms. Stable isotopes of dissolved inorganic carbon (δ^{13}C-DIC) and DO (δ^{18}O-DO) have been used to elucidate processes influencing DIC and DO concentrations in lakes (e.g., Quay et al. 1986, 1995; Herczeg 1987; Wachniew and Rozanski 1997; Wang and Veizer 2000; Luz et al. 2002; Gu et al. 2004; Myrbo and Shapley 2006; Assayag et al. 2008; Wang et al. 2008; Bass et al. 2010a, b; Karim et al. 2011; Gammons et al. 2013). These processes, reviewed by Bade et al. (2004), include advection of DIC from influent surface water or groundwater, exchange of CO_2 with the atmosphere, precipitation or dissolution of carbonate minerals, and biological reactions such as photosynthesis (P), aerobic R, sulfate reduction, and methanogenesis. For P and R, changes in the concentration and isotopic compositions of DO and DIC are inversely related. P produces DO that has the same isotopic composition as local water (which is typically depleted in ^{18}O relative to atmospheric O_2) and preferentially consumes ^{12}C-DIC over ^{13}C-DIC (Guy et al. 1993; Falkowski and Raven 1997). Thus, P causes [DO] and δ^{13}C-DIC to increase and [DIC] and δ^{18}O-DO to decrease. (here and elsewhere, brackets [] are used to denote concentration). Aerobic R has the opposite effect, producing biogenic DIC that is isotopically light (δ^{13}C ranging typically from −20 to −30 ‰; Clark and Fritz 1997) while preferentially consuming dissolved ^{16}O–^{16}O over ^{18}O–^{16}O (Angert et al. 2001). The net effect of aerobic R is, therefore, a decrease in [DO] and δ^{13}C-DIC and a concomitant increase in [DIC] and δ^{18}O-DO (Parker et al. 2005, 2010, 2014; Poulson and Sullivan 2010; Smith et al. 2011). Other biogeochemical reactions occurring in lakes may involve DO only (e.g., H_2S oxidation), DIC only (e.g., sulfate reduction or methanogenesis), or may affect both DO and DIC (e.g., aerobic methane oxidation).

Gammons et al. (2013) recently examined seasonal trends in water chemistry, δ^{18}O-DO and δ^{13}C-DIC in a deep, ultra-oligotrophic flooded mining lake in the mountains of western Montana, USA that experiences 6 months of seasonal ice cover. Although DO was depleted in the winter months

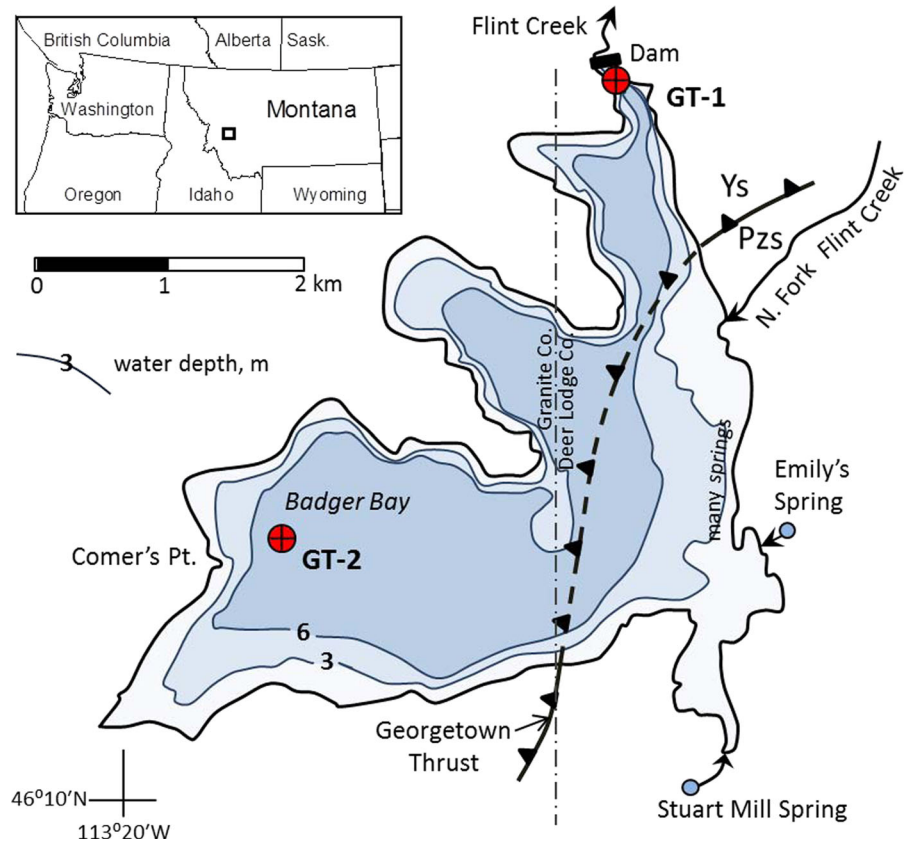

Fig. 1 Location map of Georgetown Lake. *Contours* show depth (m) of water at full pool. *Ys* mid-Proterozoic carbonate and siliclastic rocks of the Belt Supergroup, *Pzs* Paleozoic sediments, undivided (includes Mississippian Madison Group limestone)

in this low-productivity lake, most of the water column remained oxic, and vertical gradients in isotopic and chemical parameters were relatively subdued. We hypothesize that geochemical gradients and DO depletion will be much more pronounced in a shallow, highly-productive lake in a similar geographic setting that experiences a similar climate. Therefore, in the present paper we apply a combined chemical/stable isotope approach to investigate the biogeochemical cycling of DO and DIC under seasonal ice cover in Georgetown Lake, a shallow, productive, high-altitude reservoir in western Montana. Vertical and temporal changes in δ^{18}O-DO and δ^{13}C-DIC are combined with complimentary data on water isotopes and water chemistry to (1) calculate the relative rates of below-ice P and R, and (2) determine seasonal concentration changes in methane and other compounds characteristic of anoxigenic chemistry (e.g., H_2S, NH_4^+). Although this lake is known to experience DO depletion in winter (Stafford 2013), the extent of below-ice P has not previously been explored, nor has the possibility of CH_4 generation. The methods and results of this study are transferable to other shallow, fresh-water lakes in cold climates that experience seasonal ice cover.

Site description

Georgetown Lake (Fig. 1), located in western Montana at an elevation of 1,960 m, was created in 1885 by damming of a broad, grassy wetland in a high plateau surrounded by mountains. The lake was originally used for generation of hydroelectric power for nearby mining towns, but more recently has been managed as a recreational fishery as well as a source of irrigation water. Georgetown Lake contains large numbers of rainbow trout (*Oncorhynchus mykiss*), brook trout (*Salvelinus fontinalis*), and kokanee salmon (a landlocked variant of *Onchorhynchus nerka*), and is one of the most heavily recreated water bodies for its size in Montana. The shoreline is currently experiencing deforestation, in part from rapid housing development, and in part from invasion of the mountain pine beetle (*Dendroctonus ponderosae*) which has decimated pine

forests throughout the northern Rocky Mountain region (Kurz et al. 2008).

At full pool, Georgetown Lake has a surface area of 1,220 ha, a mean depth of 4.9 m, a maximum depth of 10.7 m, and a volume of 6.0×10^7 m^3 (data from Knight 1981). The surrounding watershed (13,500 ha) is elongate in a north–south direction, with peaks ranging up to 3,200 m in elevation. The North Fork of Flint Creek drains the northern highlands, and exhibits a large range in flow between spring snowmelt and baseflow conditions. The southern area is drained by Stuart Mill Spring, a large natural spring with a year-round flow of approximately 0.5 m^3/s that emerges 300 m from the SE corner of the lake. Numerous smaller springs are evident along the eastern shore, including Emily's Spring (Fig. 1). Geologically, the lake can be divided into a western half underlain by the "Middle Carbonate" metasedimentary unit of the mid-Proterozoic Belt Supergroup, and an eastern half underlain by Paleozoic sediments, including thick limestone units of the Mississippian-aged Madison Group (Lonn et al. 2003). These two rock sequences are separated by the Georgetown Thrust, a low-angle, west-dipping reverse fault. The Madison limestone is an important karst aquifer in Montana, and is the probable bedrock source for many of the springs surrounding the eastern and southern shore of the lake. Previous sampling of shallow groundwater wells around the perimeter of Georgetown Lake (Shaw et al. 2013) show that these waters are well-oxygenated, pH-neutral, Ca–Mg–HCO_3^- waters with specific conductivity (SC) between 156 and 553 µS/cm (average 326 µS/cm).

Georgetown Lake is highly productive and a lush growth of submerged macrophytes, including white-stemmed pondweed (*Potamogeton praelongus*), up to 5 m in height dominate the lake bottom. Many of these aquatic plants die back to their root stalks during the course of the winter. A number of previous studies have investigated nutrient and DO cycling in the lake (US Environmental Protection Agency, USEPA 1976; Garrison 1976; Knight 1981; Garrett 1983; Trabert 1993; Stafford 2013). Whereas the lake is well-mixed in the summer and fall due to strong winds, the water column becomes stratified in winter, with decreases in DO concentration occurring that worsen with depth and with time during the ice-covered season. Ice typically forms in mid-November and may not leave the lake until mid-May. In addition, the lake may accumulate up to a meter of snow on top of ice. Recent monitoring (Stafford 2013) suggests that Georgetown Lake is undergoing a decadal trend to more pronounced hypoxia in late winter, although the reasons for this trend remain obscure.

Methods

Sample collection

Fourteen sampling events were conducted at Georgetown Lake between November 2010 and August 2011. Water samples were collected near the dam (GT-1) at the deepest spot in the lake (46°12.852′ N/113°16.785′ W), and in Badger Bay (GT-2), 360 m northeast of the shore at a fishing access known as Comer's Point (46°10.895′ N/113°18.802′ W). Each site was chosen based on historical and concurrent monitoring by other groups. Sampling was conducted between 11:00 and 14:00, during the warmest time of the day.

A Hydrolab MS5 datasonde or an In Situ Troll 9000 datasonde was used to measure pH, oxidation–reduction potential (ORP), DO concentration [DO], water temperature (T_w), and SC. The datasondes were calibrated to the manufacturer's instructions on the morning of each sampling event using appropriate standards for the pH, ORP, and SC electrodes and water-saturated air (corrected to ambient barometric pressure) for the luminescent DO probe. The approximate accuracy of the field readings were ±0.1 pH units, ±5 mV (ORP), ±0.2 mg/L (DO), ±0.1 °C (T_w) and ±3 µS/cm (SC). For vertical profiling, the datasondes were lowered slowly into the water column with measurements taken at a vertical spacing of 0.3–0.6 m. Measurements at selected depths were repeated in reverse order when the datasonde was retrieved. A light detector (LI-192, LI-COR) was used to measure the photosynthetically active radiation (PAR) flux (400–700 nm, µmol/m^2/s). In April 2011, a Hydrolab was deployed less than 1 m below the ice for 48 h to test for diel variation in field parameters.

Water samples were retrieved from discrete depths using a submersible, 12 V pump and thick-walled plastic hose at a rate of 5–20 L/min. At least 50 L of water was pumped from each depth before any samples were taken. Samples requiring filtration were

passed through a 0.2 μm PES syringe filter using a 60 mL syringe. Samples for alkalinity titration were collected unfiltered and without preservatives in 250 mL high density polyethylene (HDPE) bottles. Filtered and acidified (1 % HNO_3) samples for metals analysis were collected in 60 mL HDPE bottles. Filtered and non-acidified samples for analysis of nutrients and anions were collected in 60 mL HDPE bottles. Samples for analysis of $\delta^{18}O$ and δD of water were filtered and collected with no head space in 10 mL glass vials with caps containing conical inserts. Samples for $\delta^{13}C$ analysis of DIC were filtered into 125 mL glass bottles with no head space. DIC was precipitated as $SrCO_3$ back in the lab by addition of $SrCl_2/NH_4OH$ solution, keeping the bottles tightly capped with no head space (Usdowski et al. 1979). Samples for $\delta^{18}O$ analysis of DO were collected by puncturing the septum of a pre-evacuated, 125-mL glass serum bottle with a needle through which a steady stream of sample water was passed (Wassenaar and Koehler 1999; Smith et al. 2011). The serum bottles were immersed in a bucket of water while they were filled, and were pre-loaded with 50 μL of saturated $HgCl_2$ as a bactericide. All sample bottles were stored on ice or in a refrigerator prior to analysis.

Three samples for $\delta^{34}S$ analysis of dissolved sulfide were collected near the bottom of the water column at GT-2 in February and March of 2011, and again in April of 2013, following the procedures of Carmody et al. (1998). Aqueous sulfide was extracted immediately after sample recovery as Ag_2S by direct addition of silver nitrate solution to a 4 L Nalgene bottle filled with lake water. This precipitate was later filtered and purified with NH_4OH to remove traces of AgCl. In addition, samples of water from Stuart Mill Spring, the North Fork of Flint Creek, and Georgetown Lake at GT-2 at a depth of 1 m were collected for $\delta^{34}S$ and $\delta^{18}O$ analysis of dissolved sulfate. Because of the low sulfate concentrations it was necessary to take 20 L of each sample and evaporate to 1 L. The evapoconcentrated solutions were filtered (0.2 μm) to remove calcite and the pH was adjusted to <2 with addition of HCl. The waters were warmed to 60 °C and a 3× excess of $BaCl_2$ solution was added to precipitate all aqueous sulfate as $BaSO_4$ (Carmody et al. 1998).

Certain trends in $\delta^{13}C$-DIC with depth (discussed below) provided indirect evidence for methanogenesis near the sediment–water interface. To test this hypothesis, several sets of samples from the bottom of the water column at GT-2 were collected for CH_4 analysis during the winter of 2013. These samples were collected using pre-evacuated glass bottles, in the same manner as described above for quantification of $\delta^{18}O$-DO.

Analytical methods

Alkalinity was measured in the laboratory within 24 h of sample collection by titrating 100.0 mL of raw, unfiltered sample with a HACH digital titrator, 1.6 N sulfuric acid cartridges, and bromcresol green-methyl red indicator dyes. Precision using this method was estimated at 2 % based on replicate titrations. Filtered, unpreserved samples were analyzed for total dissolved ammonia ($NH_4^+ + NH_3$) and soluble reactive phosphorus (SRP) within 12 h of collection using a HACH portable spectrophotometer and HACH methods 8048 (detection limit 0.3 μM) and 8038 (detection limit 1.4 μM), respectively. During the February sampling, a strong odor of H_2S was noted for samples collected at the bottom of the lake at GT-2. For future samplings, bottles and reagents were brought into the field for collection and stabilization of dissolved sulfide using the methylene blue method (HACH method 8131). 25 mL of freshly pumped water was pipetted into a polyethylene bottle and the sulfide reagents were immediately added. The concentration of total S^{2-} ($H_2S + HS^-$) was quantified in the laboratory by colorimetry within 12 h of sample collection.

A subset of samples from GT-1 and GT-2 were analyzed for major and trace elements by inductively-coupled plasma atomic emission spectroscopy (ICP-AES) and for major anions by ion chromatography (IC) at the Environmental Biogeochemistry Laboratory, University of Montana.

Most of the stable isotope analyses were performed at the University of Nevada-Reno using a Micromass Isoprime stable isotope ratio mass spectrometer (IRMS) interfaced to either a Micromass MultiPrep device or a Eurovector elemental analyzer. Samples for $\delta^{18}O$-H_2O, δD-H_2O, $\delta^{13}C$-DIC, $\delta^{18}O$-DO, $\delta^{18}O$-SO_4, and $\delta^{34}S$-H_2S/SO_4 measurement were analyzed after Epstein and Mayeda (1953), Morrison et al. (2001), Harris et al. (1997), Wassenaar and Koehler (1999), Kornexl et al. (1999), and Giesemann et al. (1994), respectively. Isotope values are reported in units of per mil (‰) in the usual δ-notation versus VSMOW for oxygen and hydrogen, VPDB for carbon,

and VCDT for sulfur. Replicate analyses indicated a reproducibility of ±0.1 ‰ for $\delta^{18}O$-H_2O, ±1 ‰ for δD-H_2O, ±0.05 ‰ for $\delta^{13}C$-DIC, ±0.1 ‰ for $\delta^{18}O$-DO, ±0.4 ‰ for $\delta^{18}O$-SO_4, and ±0.2 ‰ for $\delta^{34}S$-H_2S and $\delta^{34}S$-SO_4. A single sample of water from the bottom of the water column at GT-2 collected in April 2013 was analyzed for $\delta^{13}C$-CH_4 using a Picarro cavity ring-down spectrometer at Montana State University. The $\delta^{13}C$ analysis was performed in triplicate, using three different dilution factors, and returned a precision of ±0.3 ‰.

Samples for CH_4 analysis were collected in 125 mL pre-evacuated serum bottles as previously described. A small headspace was created in these bottles due to exsolution of dissolved gasses. This headspace was sampled in the laboratory by puncturing the septum with a gas-tight syringe and withdrawing a gas sample (usually 20 µL) followed by analysis using a Thermo Scientific Trace GC Ultra with a TracePLOT TG-BOND Msieve 5A column connected to a Thermo Scientific ITQ 900 mass spectrometer using electron ionization. The GC method used UHP-He carrier gas, an inlet temperature of 250 °C, a split ratio of 60, split flow of 18, 0.3 mL/min constant column flow, 30 °C isothermal column temperature, outlet temperature of 250 °C and an ion source temperature of 250 °C. Calibration was performed using a standard mixture containing O_2, N_2, CO_2, CO, CH_4 and the balance being He (Scotty #501697). Solution concentrations of CH_4 were determined using the methane solubility equations of Wiesenburg and Guinasso Jr (1979). The pre-sampling CH_4 concentration was determined by mass balance calculations based on the sum of the CH_4 in the headspace, the moles of CH_4 in solution, and the total sample and headspace volumes, which were determined gravimetrically.

Geochemical modeling

DIC was speciated using the program Visual MINTEQ, version 3.0 (a recent adaption of the original program described by Allison et al. 1991) based on the measured pH, alkalinity, and T_w of each sample. Calculated charge imbalances were used as a quality control check: in most cases the charge imbalance was less than 5 %. Visual MINTEQ was also used to calculate CO_2 partial pressures and mineral saturation indices (SIs). Selected results are discussed below.

Results

Water isotopes and lake hydrology

The isotopic composition of water samples collected from Stuart Mill Spring and the North Fork of Flint Creek in November 2010 and June 2011 (Fig. 2a) fall close to the global meteoric water line (MWL), indicating that minimal evaporation occurred prior to entering Georgetown Lake (data in Supplementary Material). In contrast, all of the lake samples collected between November 2010 and March 2011 were moderately evaporated, and define a local evaporation line (LEL) with the following equation: $\delta D = 4.86 \times \delta^{18}O - 49.2$ ($R^2 = 0.979$). The slope of this line correlates to an average relative humidity of roughly 65 %, and is very close to the slope of the LEL for nearby Butte, Montana (slope = 5.0, Gammons et al. 2006). The maximum shift in $\delta^{18}O$ away from the MWL for the most evaporated samples was approximately 4 ‰, consistent with up to 10–15 % loss of water to evaporation (Gammons et al. 2006). Much of this evaporation presumably occurred during the preceding ice-free period in the summer and fall of 2010.

Although the isotopic compositions of water samples at GT-1 and GT-2 were similar in November of 2010, the two sites had quite different stable isotope profiles in March 2011 (Fig. 2b). GT-2 showed a slight increase in $\delta^{18}O$ and δD with depth in the lake, whereas GT-1 showed a distinct shift to lighter isotopic values with depth. The latter trend is tentatively explained by mixing of isotopically light groundwater entering the lake from submerged springs along the eastern shore of Georgetown Lake. Previous work (Shaw et al. 2013) characterized the east shore of the lake as a groundwater discharge zone based on spatial trends in dissolved radon gas. In contrast, the western bays of the lake, including Badger Bay, showed no evidence of influent groundwater.

Field parameters

In early November 2010, before the onset of ice cover, the water columns were well-mixed at both GT-1 and GT-2, and both stations had similar values of temperature, SC, and [DO]. Ice formed in late November, and by the next sampling date in December both stations were stratified, with an increase in temperature and SC and a decrease in [DO] with depth (Figs. 3, 4). These

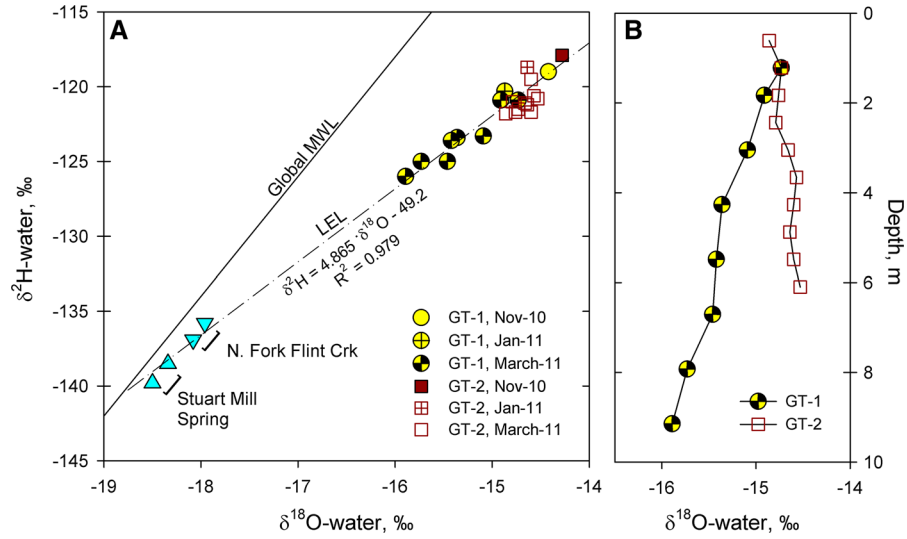

Fig. 2 Water isotope results. **a** Isotope cross-plot: the global meteoric water line (MWL) is from Craig (1961), and the local evaporation line (LEL) is a regression of data from this study. **b** Variations in water-$\delta^{18}O$ with depth at GT-1 and GT-2 in March 2011

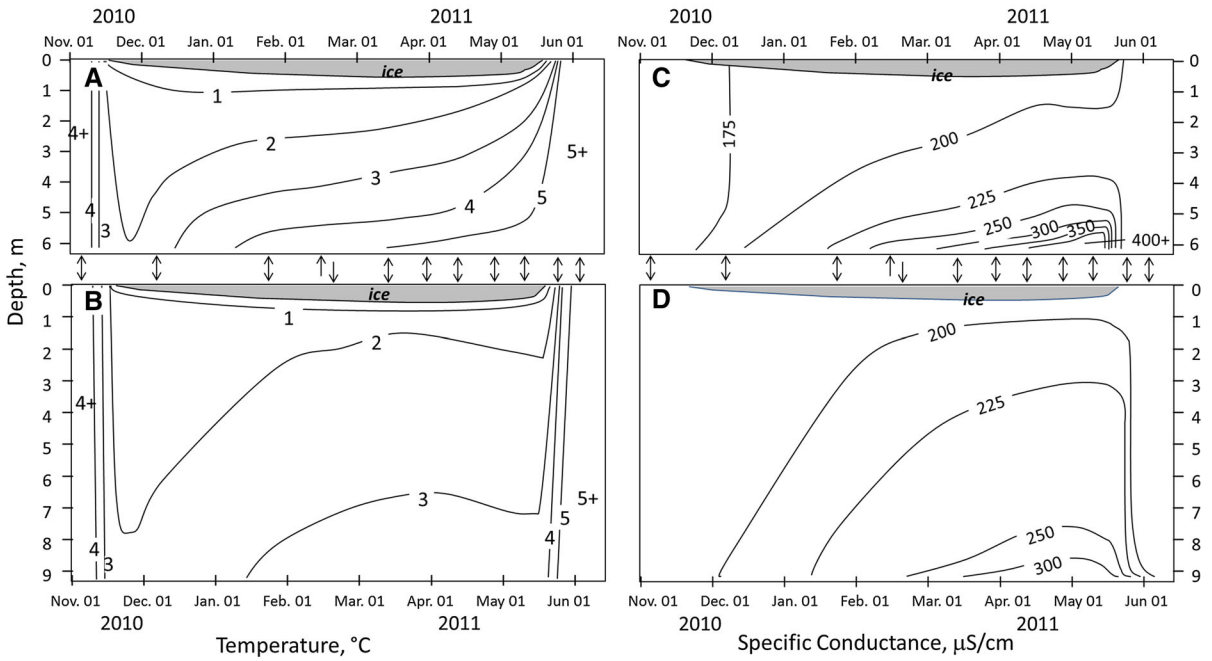

Fig. 3 Changes in water temperature (**a**, **b** *contours* in °C) and specific conductance (**c**, **d** *contours* in µS/cm) with depth and time. **a**, **c** GT-2 (Badger Bay), **b**, **d** GT-1 (dam). *Contour lines* were generated with Golden Software's Surfer program. *Arrows* in *centerline* of figure denote dates when *vertical* profiles were collected at GT-2 (*arrow up*), GT-1 (*arrow down*) or both sites (*arrow* both directions)

trends magnified with time until ice-off occurred on 24–26 May 2011, after which point strong winds induced vertical mixing. Vertical profiles obtained on 5 June and 11 August 2011 showed minimal changes in SC and [DO] with depth at both sites (Figs. 3, 4). This is consistent with studies performed in the 1980s (Knight 1981) and more recently (Stafford 2013) which show that Georgetown Lake is vertically mixed throughout the non-frozen months.

The GT-2 site in Badger Bay showed an increase in SC with depth, especially near the bottom of the lake, which became more pronounced as the winter

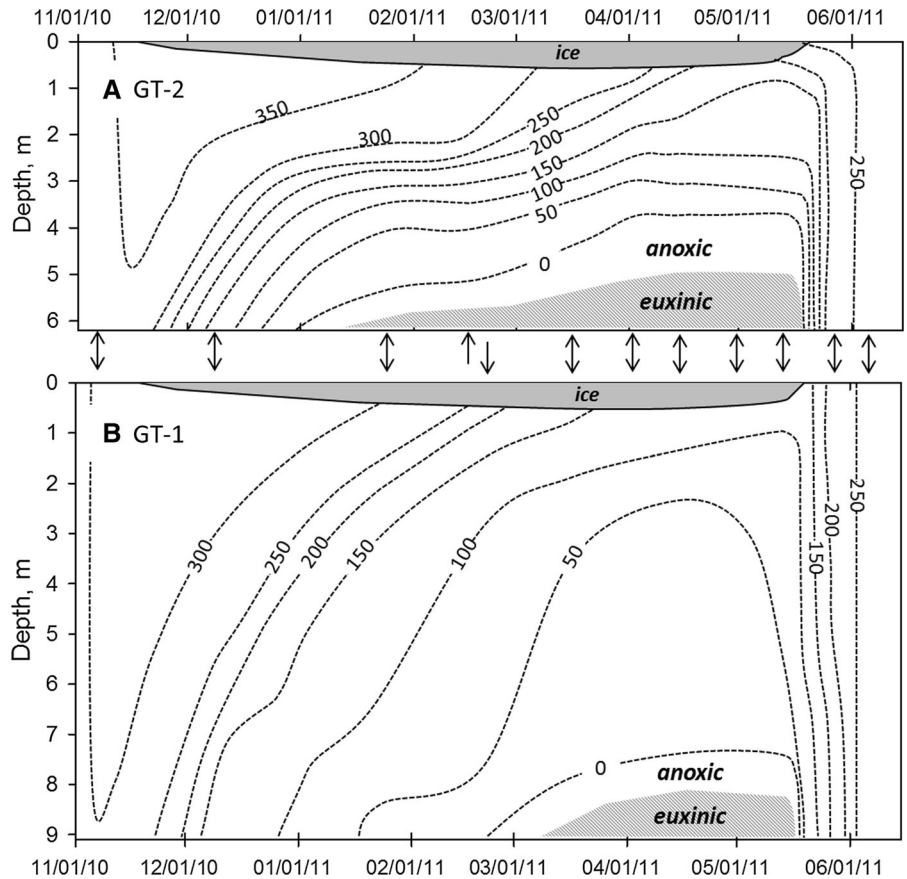

Fig. 4 Changes in dissolved oxygen concentration (*contours* in μM) with depth and time. **a** GT-2 (Badger Bay), **b** GT-1 (dam). *Contour lines* were generated with Golden Software's Surfer program. The *hatched area* indicates the presence of H_2S. *Arrows* in *centerline* of figure denote dates when *vertical* profiles were collected at GT-2 (*arrow up*), GT-1 (*arrow down*) or both sites (*arrow* both directions)

progressed (Figs. 3, 4). As discussed below, most of this change in SC is believed to have been caused by diffusion of solutes, especially Ca^{2+} and HCO_3^-, from sediment pore-water. Both GT-1 and GT-2 developed a deep anoxic layer which increased in thickness as the winter progressed. This anoxic layer was thicker and set up earlier in the winter at GT-2 compared to GT-1 (Fig. 4). Nonetheless, a layer of oxic water in the overlying water column maintained sufficient [DO] for trout and salmon to overwinter in Badger Bay. In contrast, [DO] in shallow water at GT-1 dropped to values <150 μM, and most of the water column had [DO] <100 μM, which would have caused severe stress for trout (Raleigh et al. 1984).

Chemistry

The water columns at GT-1 and GT-2 were highly stratified in March 2011, with a nearly 3-m thick anoxic layer extending from mid-depth to the sediment–water interface (Fig. 5). PAR decreased in the top several meters, but was still detectable (0.1–0.6 μmol/s/m^2 in the bottom meter of the water column (Fig. 5b, g). On the day of PAR measurement, the lake had approximately 0.8 m of ice and 0.2 m of compact, windblown snow cover. An increase in SC towards the bottom of the lake at GT-2 was highly correlated (R^2 >0.98) with a parallel increase in [HCO_3^-] (Fig. 5c). The GT-1 profile shows a more gradual increase in SC and [HCO_3^-] with depth (Fig. 5h). Despite the increase in [HCO_3^-], pH decreased towards the bottom of the lake at both sites (Fig. 5a, f) due to an even greater increase in [CO_2] (Fig. 5e, j).

Bicarbonate ion is by far the dominant anion in Georgetown Lake, with concentrations in the 1–2 mM range, compared to <0.05 mM for SO_4^{2-} and Cl^-. Cations are dominated by Ca^{2+} and Mg^{2+}. Whereas [Mg^{2+}] showed no change with depth in March 2011, [Ca^{2+}] increased sharply near the sediment–water interface at GT-2 (Fig. 5e), and to a

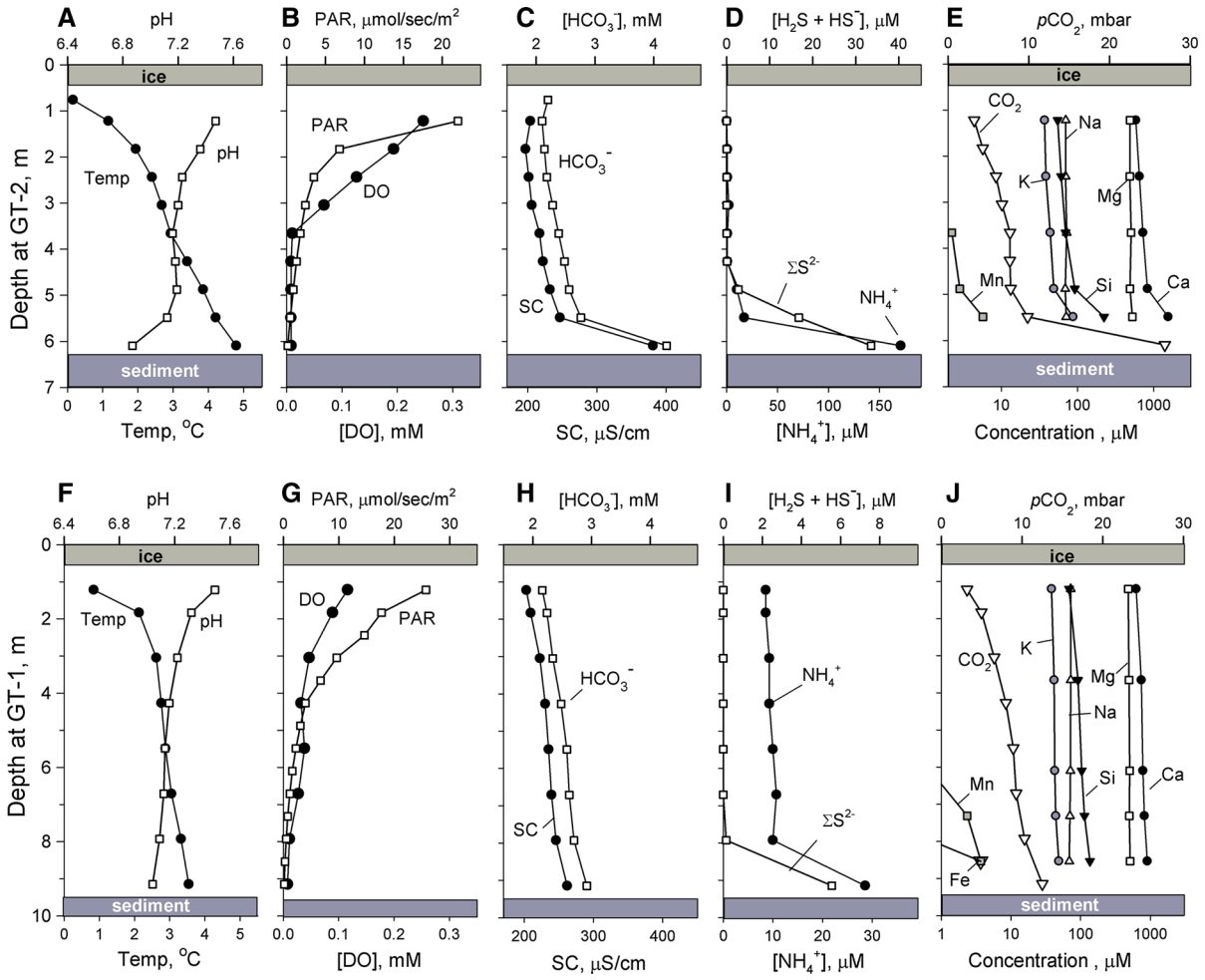

Fig. 5 Example *vertical* profiles in selected water column properties at GT-1 (*bottom row*) and GT-2 (*top row*) for March 2011. Water temperature and pH (**a**, **f**), photosynthetically active radiation (PAR) and dissolved oxygen (DO; **b**, **g**), specific conductance (SC) and bicarbonate ion (**c**, **h**), ammonium (NH_4^+) and dissolved sulfide (**d**, **i**), other major and trace solutes (**e**, **j**). All concentration scales are linear, except for logarithmic concentration *scales* for other major and trace solutes (**e**, **j**)

lesser extent at GT-1 (Fig. 5j). Amongst the remaining solutes, K^+ and dissolved SiO_2 increased in concentration towards the bottom of the lake (Fig. 5e, j), whereas Na^+ and Mg^{2+} did not. Concentrations of most trace metals were below the analytical detection limit of the ICP-AES. Exceptions include Mn, which was detected in the deep water samples on most sampling dates (Fig. 5e, j), and Fe, which was detected in the deep water at GT-1 (Fig. 5j), but not GT-2 (Fig. 5e).

Concentrations of dissolved NO_3^- were below the detection limit of the IC (5 µM) for all samples analyzed in this study. In contrast, $[NH_4^+]$ increased towards the bottom of the lake in late winter, to >25 and >150 µM at GT-1 and GT-2, respectively (Fig. 5d, i). Concentrations of soluble reactive phosphate (SRP) were below detection except near the bottom of the water column where [SRP] exceeded 0.5 µM at both sampling sites (data in Supplementary Material).

To test the hypothesis that methanogenesis was occurring near the sediment–water interface, several samples were taken in 2013 for quantification of dissolved CH_4. A sharp rise in $[CH_4]$ was documented near the bottom of the water column at GT-2 on all dates sampled (Table 1). Maximum concentrations of CH_4 were in the range of 500–1,000 µM in January, February and March of 2013.

Table 1 Concentrations of dissolved CH_4 in samples from GT-2

Dates	Depth (m)	Temperature (°C)	[DIC] (mM)	δ^{13}C-DIC (‰)	[CH_4] (μM)
26 January 2013	5.79	4.69	na	na	16
	6.40	4.76	na	na	595
16 February 2013	4.42	4.39	3.79	na	24
	5.64	4.60	3.54	na	44
	6.25	4.34	10.8	na	695
29 March 2013	4.27	4.36	4.85	−5.4	25
	4.88	4.46	5.21	−6.1	72
	5.49	4.69	5.11	−5.2	121
	6.10	5.36	17.3	−1.1	1,020

na Not analyzed

Table 2 Concentrations and isotopic compositions of dissolved oxygen (DO)

GT-1 dam site				GT-2 Badger Bay			
Depth (m)	[DO] (μM)	[DO] (% sat)	$\delta^{18}O_{DO}$ (‰)	Depth (m)	[DO] (μM)	[DO] (% sat)	$\delta^{18}O_{DO}$ (‰)
6 November 2010							
0.3	302	95.2	16.0	0.3	316	99.1	17.6
3.0	302	95.0	15.7	2.4	316	99.0	18.2
6.1	301	94.6	16.2	4.6	319	99.7	17.7
24 January 2011							
1.5	251	70.1	22.6	1.5	334	63.4	20.5
3.0	152	43.4	24.5	2.7	191	54.5	22.4
4.6	117	33.6	26.2	3.7	67	22.0	20.6
6.1	101	29.0	25.6				
7.6	77	22.6	26.9				
8.8	41	12.0	29.3				
16 March 2011							
1.2	116	33.4	26.8	0.6	270	74.0	21.4
1.8	89	25.9	29.0	1.2	246	70.0	22.0
3.0	47	13.7	32.6	1.8	193	55.6	22.3
4.3	32	9.5	31.3	2.4	126	36.8	22.9
5.5	38	11.4	33.2				

Isotopes of DO and DIC

Prior to ice-on, values of δ^{18}O-DO were similar at GT-1 (average 16.0 ‰) and GT-2 (average 17.8 ‰), and showed no clear changes with depth (Table 2; Fig. 6a, b). Both sites had δ^{18}O-DO values significantly lower than the expected value of 24.2 ‰ for DO in equilibrium with atmospheric O_2 (Benson and Krause Jr 1980). Once ice cover was established, δ^{18}O-DO increased with both depth and time, and these trends were magnified at the GT-1 site. No isotopic data are available for DO in the deeper portions of the water columns at GT-1 and GT-2, due to insufficient DO concentrations for IRMS analysis. Overall, δ^{18}O-DO values increased with decreased [DO]. However, the slope of the relationship was considerably steeper for the GT-1 data set compared to GT-2 (Fig. 7). Possible reasons for these differences are discussed below.

Spatial and temporal changes in δ^{13}C-DIC under ice cover (Table 3; Fig. 6c, d) show more complexity

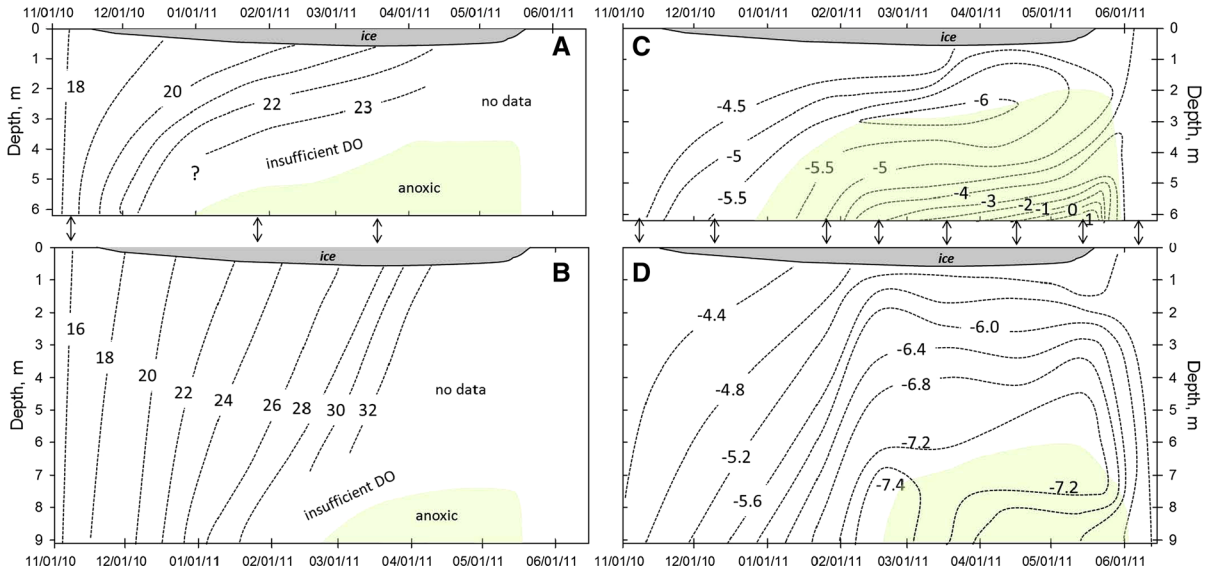

Fig. 6 Spatial and temporal trends in the isotopic composition of dissolved oxygen (**a**, **b**) and dissolved inorganic carbon (**c**, **d**) at GT-2 (**a**, **c**) and GT-1 (**b**, **d**). *Shaded areas* in **a** and **b** show depths where [DO] was absent (based on data in Fig. 4). *Shaded areas* in **c** and **d** represent the portion of the water column where δ^{13}C-DIC increased with depth. *Contour lines* were generated with Golden Software's Surfer program. *Arrows* in *centerline* of figure denote dates when samples were collected for isotopic analysis of DO or DIC at both sites

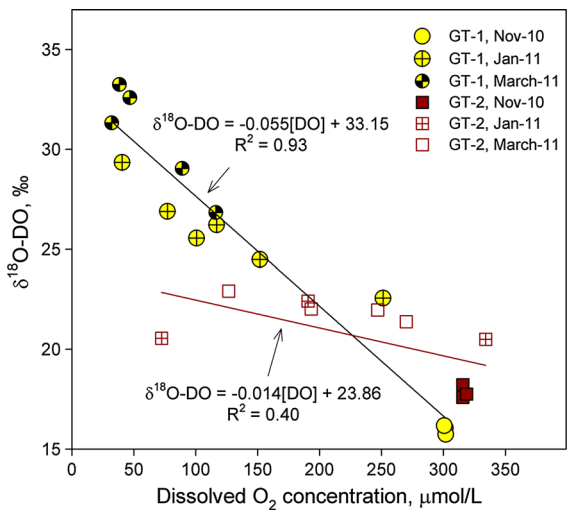

Fig. 7 The isotopic composition of dissolved oxygen (δ^{18}O-DO) versus DO concentration at GT-1 (*circles*) and GT-2 (*squares*). Linear regressions are for all data from each respective site

than the changes in δ^{18}O-DO outlined above. Prior to development of ice, both GT-1 and GT-2 had similar values of δ^{13}C-DIC, near −4.3 to −4.5 ‰. Early in the winter, there was a clear trend at both sites of a decrease in δ^{13}C-DIC with both depth and time. However, by early January this trend reversed in the deeper water at GT-2; at GT-1, a similar reversal was observed by early March (see shaded regions in Fig. 6c, d). The deepest water at GT-2 showed a dramatic increase in δ^{13}C-DIC to values greater than +1 ‰, whereas the analogous increase was more subtle at GT-1. The increase in δ^{13}C-DIC at depth coincided with substantial increases in [DIC] (Fig. 8). Possible sources of this influx of isotopically heavy DIC are discussed below. Following ice-off in late May, most of the changes in δ^{13}C-DIC with depth were homogenized due to mixing of the water column.

Isotopes of sulfide and sulfate

Similar to NH_4^+ and SRP, concentrations of dissolved sulfide increased sharply near the base of the water column at both GT-1 and GT-2 (Fig. 5d, i), presumably from bacterial sulfate reduction (BSR) in the shallow sediment, possibly augmented by putrefaction of organic-S in decaying plants or animals (Dunnette et al. 1985). The concentration of dissolved sulfide at GT-2 at 6 m depth (30–60 μM) was similar to that of dissolved sulfate at 1 m depth on the same day (Table 4). Euxinic bottom water at GT-2 collected on

Table 3 Concentrations and isotopic compositions of dissolved inorganic carbon (DIC) in Georgetown Lake and influent waters

GT-1 dam site			GT-2 Badger Bay			GT-1 dam site			GT-2 Badger Bay		
Depth (m)	[DIC] (mM)	$\delta^{13}C_{DIC}$ (‰)	Depth (m)	[DIC] (mM)	$\delta^{13}C_{DIC}$ (‰)	Depth (m)	[DIC] (mM)	$\delta^{13}C_{DIC}$ (‰)	Depth (m)	[DIC] (mM)	$\delta^{13}C_{DIC}$ (‰)
6 November 2010			6 November 2010			15 April 2011			15 April 2011		
0.3	1.93	−4.6	0.3	1.69	−3.9	1.2	2.93	−5.5	1.2	2.84	−5.5
3.0	1.83	−4.4	2.4	1.75	−3.9	3.0	3.39	−6.2	2.4	2.96	−6.0
6.1	1.85	−4.4	4.6	1.74	−3.9	4.3	3.52	−6.9	3.7	3.00	−5.7
8 December 2010			8 December 2010			6.1	3.71	−6.8	4.9	3.50	−4.4
0.3	2.03	−4.2	0.3	1.95	−4.0	7.9	3.79	−6.8	5.5	4.20	−3.5
4.0	2.10	−4.6	2.7	1.87	−4.1	9.1	4.23	−6.5	6.1	6.54	+0.8
7.6	2.49	−5.2	4.6	2.19	−5.0	13 May 2011			13 May 2011		
24 January 2011			24 January 2011			0.6	1.23	−4.7	1.2	3.02	−5.3
1.5	2.16	−4.7	1.5	1.97	−4.2	1.8	3.17	−5.6	2.4	3.18	−5.5
3.0	2.45	−5.3	2.7	2.16	−5.2	3.0	3.51	−6.7	3.7	3.55	−5.1
4.6	2.63	−5.6	3.7	2.31	−5.1	4.3	3.70	−7.2	4.9	3.82	−3.9
6.1	2.72	−6.1	5.5	2.56	−5.5	5.5	3.80	−7.5	6.1	7.83	+1.7
7.6	2.80	−6.7				6.7	3.95	−7.5			
8.8	2.97	−6.9				7.9	4.20	−7.1			
15 February 2011			15 February 2011			9.1	4.99	−6.2			
1.2	2.18	−5.5	1.2	na[a]	−4.8	5 June 2011			5 June 2011		
2.1	2.32	−6.1	1.8	na	−4.8	1.5	2.56	−5.5	1.8	2.85	−5.4
3.0	2.42	−6.1	2.4	na	−5.2	4.6	2.52	−5.7	3.7	2.86	−3.8
4.0	2.52	−6.6	3.0	na	−6.0	7.6	2.56	−6.0	5.5	2.87	−3.8
4.9	2.57	−6.9	3.7	na	−5.5	11 August 2011			11 August 2011		
5.8	2.68	−6.8	4.3	na	−5.4	0.3	1.85	−4.7	0.3	1.85	−3.8
6.7	2.75	−7.6	4.9	na	−5.4	3.0	1.89	−4.4	3.0	1.84	−3.5
7.6	2.84	−7.7	5.5	na	−0.6	6.1	1.88	−4.5	5.6	1.79	−3.8
8.5	2.94	−7.9				9.1	1.91	−4.6			
16 March 2011			16 March 2011			Miscellaneous surface samples					
1.2	2.39	−5.3	0.6	2.57	−4.5	6 November 2010					
1.8	2.59	−5.7	1.2	2.34	−4.2	Stuart Mill Spring				2.96	−11.1
3.0	2.79	−6.4	1.8	2.45	−4.9	North Fork of Flint Creek				2.39	−9.1
4.3	3.03	−6.9	2.4	2.60	−5.6	Emily's Spring				3.14	−10.1
5.5	3.19	−7.1	3.0	2.74	−5.5	2 August 2011					
6.7	3.25	−7.3	3.7	2.91	−5.0	Stuart Mill Spring				3.19	−10.9
7.9	3.40	−7.5	4.3	3.00	−4.9	North Fork of Flint Creek				2.32	−10.1
9.1	3.76	−7.2	4.9	3.08	−4.6						
			5.5	3.41	−4.3						
			6.1	5.95	−0.1						

[a] Total DIC not available due to pH meter malfunction

three different dates had $\delta^{34}S\text{-}H_2S$ in the range of +4.8 to +8.5 ‰ (Table 4). This compares to a single value of +9.7 ‰ for $\delta^{34}S$ of aqueous sulfate in the shallow water at GT-2 (Table 4). Whereas the two main tributaries to the lake had $\delta^{18}O\text{-}SO_4$ values of +2.8 ‰ (Stuart Mill Spring) and +0.8 ‰ (North Fork of Flint Creek), sulfate in the shallow water at GT-2 was depleted in ^{18}O (−6.4 ‰).

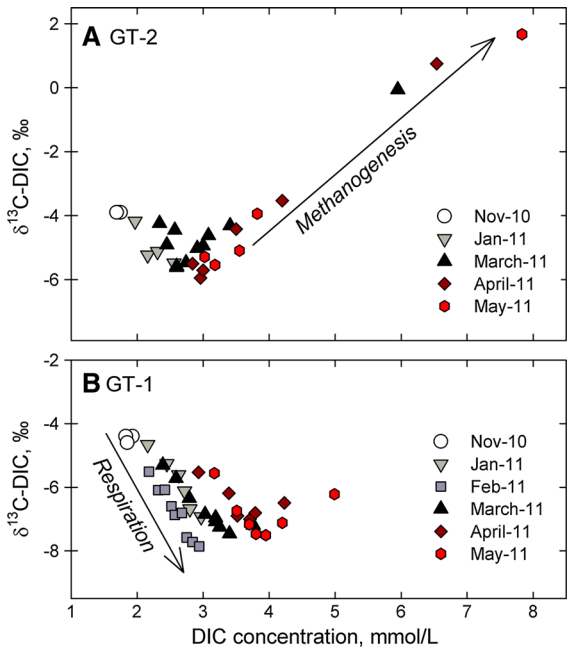

Fig. 8 The isotopic composition of dissolved inorganic carbon (δ^{13}C-DIC) versus DIC concentration at GT-2 (**a**) and GT-1 (**b**). *Arrows* show inferred trends for respiration (negative slope) and methanogenesis (positive slope)

Discussion

Controls on lake chemistry

The establishment of vertical gradients in water chemistry under ice cover could be attributed to several processes, including: (1) inputs of groundwater, (2) solute exclusion during ice formation, and (3) upward diffusion of solutes from the sediment–water interface.

In addition to Stuart Mill Spring, Georgetown Lake receives a significant amount of groundwater in the form of submerged springs, especially along the eastern shore of the lake. Shaw et al. (2013) showed that dissolved radon concentrations in Georgetown Lake under ice cover were elevated along the eastern shore, but not in the western portion of the lake (e.g., near GT-2). This radon was inferred to come from upwelling groundwater. Based on sampling of domestic water wells, groundwater to the east of the lake is Ca–Mg–HCO_3 type, oxidized (DO present), with an average SC of 326 µS/cm. Groundwater entering the lake in winter would therefore tend to sink (higher density than most of the water column of the lake). Consistent with this idea, stable isotope profiles from March 2011 (Fig. 2) show evidence of mixing of deep, non-evaporated water (i.e., groundwater) with evaporated lake water at GT-1, but not at GT-2. Despite mixing of presumably oxidized groundwater into the water column along the eastern shore of the lake, the biological and chemical oxygen demand of the sediment and overlying stratified water column was more than sufficient to maintain anoxic conditions for deep water by the time it reached the dam outlet. Because the outlet pipes draw water from the bottom of the lake, water that is discharged has a chemistry that matches that of deep water at GT-1. This includes the presence of H_2S, which, in late winter, imparts a strong odor to Flint Creek in the first several hundred meters below the dam.

Solute exclusion during freezing of water to ice is another process that could influence the chemistry of Georgetown Lake. For water bodies with high salinity (e.g., some Antarctic lakes and marine estuaries) this process, termed thermohaline convection, can lead to

Table 4 Isotopic compositions of dissolved sulfate and sulfide

Dates	Locations	Depth (m)	$[\Sigma S^{2-}]$ (µM)	δ^{34}S-H_2S (‰)	$[SO_4^{2-}]$ (µM)	δ^{34}S-SO_4^{2-} (‰)	δ^{18}O-SO_4^{2-} (‰)
15 February 2011	GT-2	6.1	47	4.8	na	na	na
16 March 2011	GT-2	5.9	34	8.5	na	na	na
24 April 2013	GT-2	6.1	56	6.4	na	na	na
24 April 2013	GT-2	2.1	na	na	50	9.7	−6.4
24 April 2013	Stuart Mill Spring	0	na	na	31	13.6	2.8
24 April 2013	North Fork of Flint Creek	0	na	na	31	4.7	0.8

na Not analyzed

permanent meromixus (Gibson 1999). In Georgetown Lake, most ice forms in December and early January. However, because of the low salinity of the lake, the increases in SC of the water column during early winter were relatively minor (Fig. 3). Exclusion of dissolved gas during freezing may also have temporarily increased [DO] of the shallow water, although no values of [DO] that exceeded atmospheric saturation were measured in this study.

Diffusion of solutes from the sediment pore-water is probably the dominant process leading to the deep layers of high-TDS, anoxic water at both GT-1 and GT-2. Like the overlying water column, the major ion composition of the deep water is dominated by Ca^{2+} and HCO_3^-. Inputs of Ca^{2+} and HCO_3^- from the sediment could occur from dissolution of calcite in response to elevated CO_2 partial pressure:

$$CaCO_3(s) + H_2O + CO_2(aq) = Ca^{2+} + 2HCO_3^-. \quad (1)$$

Based on thermodynamic modeling with Visual MINTEQ, all water samples collected during the period of ice cover had calcite SIs (SI = log ion activity quotient divided by the equilibrium constant) that were significantly negative. At GT-1, the SI range was −0.68 to −0.97 with an average of −0.86 ($n = 18$). At GT-2, the SI range was −0.19 to −1.18 with an average of −0.62 ($n = 13$). Thus, any calcite in sediment at the bottom of the lake should have been dissolving. Samples collected in November prior to ice formation had calcite SI values of −0.23 (GT-2) and −0.03 (GT-2), and were thus closer to equilibrium. In a previous study, Knight (1981) suggested that Georgetown Lake is typically supersaturated with calcite during the warm summer months, and undersaturated during winter.

In August 2011, a diffusion sampler (i.e., "peeper") was used to collect samples of sediment-pore water from a location in Badger Bay close to GT-2, but in shallower water (data in Shaw et al. 2013). Although the location and time of year are different, the results bear on the current study. Pore water from 10 cm below the bottom of the lake contained >400 mg/L HCO_3^-, >150 mg/L Ca^{2+}, >10 mg/L each of K^+, Fe^{2+}, NH_4–N, and Si, >3 mg/L Mn^{2+}, and >0.5 mg/L PO_4–P. Concentrations of sulfate were below detection and total dissolved sulfide was roughly 0.1 mg/L. The most likely source of K^+, NH_4–N and PO_4–P is decay of organic matter in the sediment (Shaw et al. 2013), and the high concentrations of Ca^{2+} and HCO_3^- are consistent with dissolution of calcite in an environment of high p_{CO_2}. Elevated concentrations of silica could be related to dissolution of amorphous silica in the form of diatom frustules. The somewhat elevated concentrations of Fe^{2+} and Mn^{2+} suggest reductive dissolution of hydrous Fe and Mn oxides. Finally, the presence of H_2S and absence of SO_4^{2-} is consistent with BSR.

Upward diffusion of solutes from a more concentrated sediment-pore water (as above) can explain most of the observed changes in chemistry of the deep lake under ice cover, including increases in the concentrations of Ca^{2+}, HCO_3^-, K^+, NH_4^+, PO_4–P, dissolved silica, dissolved Fe and Mn, and H_2S. The lower concentration of dissolved Fe at GT-2 (below detection) compared to GT-1 may be explained by the higher concentration of H_2S at GT-2, leading to precipitation of Fe-sulfide. Additional sampling of sediment pore water during the winter months at GT-2 is planned to quantify the diffusive flux of solutes into the overlying water column and their cumulative oxygen demand.

DO cycling under ice cover

Because of the extremely slow diffusivity of gases through ice, the only appreciable sources of DO to the water column for a shallow lake under ice cover are aquatic P and influx of oxygenated groundwater or surface water. However, there are a number of possible sinks for DO, including the aerobic microbial oxidation of organic matter (aerobic R), methane (methanotrophy), ammonium (nitrification), aqueous sulfide, and reduced metals such as Fe^{2+} or Mn^{2+}. Because of the widespread distribution of particulate organic matter, macrophytes, and higher organisms (insects, fish) in the lake, aerobic R should occur throughout the entire oxic portion of the water column. In contrast, CH_4, NH_4^+, H_2S, Fe^{2+} and Mn^{2+} are most likely generated within the sediment where they subsequently diffuse upwards into the lake and are oxidized at the oxic/anoxic interface in the water column. The production of these reduced species is likely coupled to the oxidation of organic carbon under anoxic conditions. Because the concentrations of sulfide, ammonium, and dissolved Fe/Mn are

relatively low in Georgetown Lake (Fig. 3), the main sink for DO in winter is most likely oxidation of organic C. Oxidation of methane diffusing upward out of the anoxic layer could also be an important sink for downward diffusing DO. Methane can also rise quickly to the oxic zone beneath the ice via ebullition of bubbles generated near the sediment–water interface.

P produces ^{18}O-depleted DO with a similar O-isotope composition as the surrounding water (in this case, near −16 ‰). Aerobic R fractionates O-isotopes so that δ^{18}O-DO of residual DO is shifted to heavy values as DO is consumed (Kroopnick 1975; Guy et al. 1993), as does abiotic oxidation of aqueous sulfide (Oba and Poulson 2009a), abiotic oxidation of Fe^{2+} (Oba and Poulson 2009b), consumption of O_2 by methanotrophs (Mandernack et al. 2009), and possibly the aerobic oxidation of ammonium (suggested by Mandernack et al. 2009). Assuming that R of organic C is the main sink for DO under ice cover, the residual DO pool should become progressively enriched in ^{18}O as DO concentrations diminish. This trend is clearly shown at both GT-1 and GT-2, although much more so at the deeper, GT-1 site. Previous studies have documented similar increases in δ^{18}O-DO with lake depth (Luz et al. 2002; Bass et al. 2010a; Brown and Poulson 2010; Gammons et al. 2013).

Previous workers (Quay et al. 1995; Wang and Veizer 2000) have shown that simultaneous measurement of δ^{18}O-DO and [DO] can be used to estimate the relative rates of oxygenic P and R in lakes. If the system is at steady state, and there is no net exchange of gases across the air–water interface, then the P/R ratio is given by (equations and values of constants from Wang and Veizer 2000):

$$P/R = \left(R^*_{DO}\alpha_r - X_g\right)/\left(R_W - X_g\right), \quad (2)$$

$$X_g = \alpha^*_g\left(R^*_{atm}\alpha_s - \left([DO]/[DO_{sat}]\right)^* R_{DO}\right)/(1 - [DO]/[DO_{sat}]), \quad (3)$$

where α_r is the O-isotopic fractionation from R and has typical values of 0.977–0.98 (e.g. Kroopnick 1975; Kiddon et al. 1993), although a larger range of values has been measured (e.g. Lane and Dole 1956; Brandes and Devol 1997), α_g is the ratio of ^{18}O–^{16}O to ^{16}O–^{16}O gas transfer velocities (0.9972 at 20 °C), α_s is the ratio of ^{18}O–^{16}O to ^{16}O–^{16}O solubility in water (1.0007), R_{DO} is the ^{18}O/^{16}O ratio of DO (measured), R_{atm} is the ^{18}O/^{16}O ratio of O_2 in air, R_W is the ^{18}O/^{16}O ratio of water, [DO] is the measured DO concentration, and $[DO]_{sat}$ is the computed DO concentration at atmospheric saturation at the temperature and pressure of interest. In the present study, ice creates a physical barrier to gas exchange with the atmosphere. Although the observed gradients in [DO] with time show that the lake was not at steady state with respect to DO on the time scale of weeks–months, changes in [DO] or δ^{18}O-DO were most likely negligible on the scale of hours–days. A datasonde placed in shallow water under the ice in April 2011 showed minimal change in [DO] (<3 μM) over two 24-h periods.

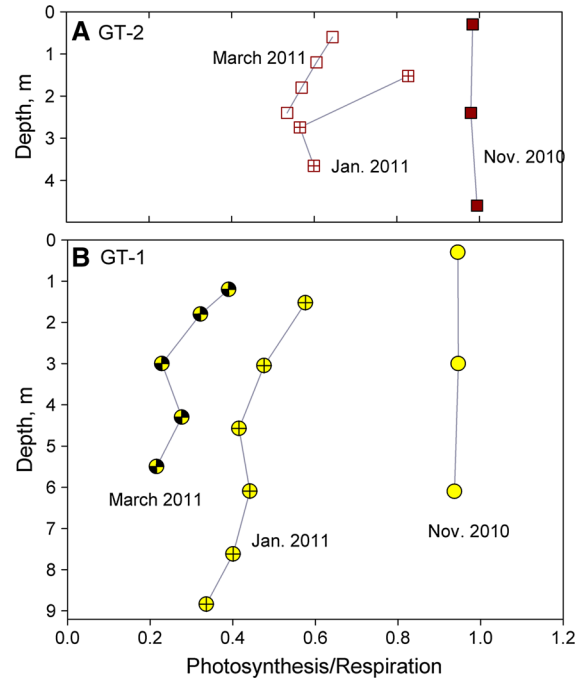

Fig. 9 Calculated photosynthesis/respiration (P/R) ratios at GT-2 (**a**) and GT-1 (**b**)

With the above steady-state caveat in mind, the P/R equations of Quay et al. (1995) and Wang and Veizer (2000) were applied to the data in this study. The results (Fig. 9) show that oxygenic P and R were almost equal (P/R $\sim$ 1) at both sites in November, prior to ice formation. Once ice formed, the expected trends were shown wherein the lake became more R-dominated with depth on any given sampling date, and also with time as winter progressed. At the same depth and sampling dates, P/R ratios were significantly higher at GT-2 than at GT-1, especially for the March 2011 data set. This result is consistent with other

observations that suggest a higher P/R ratio under ice at GT-2, including higher overall DO concentrations at shallow depth late in the season.

DIC cycling under ice cover

Internal sources of DIC in winter include production of biogenic CO_2 by aerobic or anaerobic R, methanogenesis, and dissolution of carbonate minerals. R of organic carbon—both aerobic and anaerobic—adds CO_2 to the water column with a $\delta^{13}C$ value that is similar to that of the carbon source, i.e., −20 to −30 ‰ for C3 plants in temperate climates (Clark and Fritz 1997). Methanogenesis occurs via several pathways, two of which are discussed here as each is well characterized and their effect on [DIC] and $\delta^{13}C$-DIC is well documented (Whiticar et al. 1986; Whiticar 1999). One pathway involves reduction of CO_2 by H_2:

$$CO_2 + 4H_2 \rightarrow CH_4 + 2H_2O. \quad (4)$$

Due to kinetic isotopic effects, CH_4 formed by this pathway is strongly depleted in ^{13}C, resulting in an increase in $\delta^{13}C$ of the residual DIC pool as [DIC] decreases. The second pathway, acetoclastic methanogenesis, produces a 1:1 mixture of isotopically-heavy DIC (as HCO_3^-) and isotopically-light CH_4:

$$CH_3COO^- + H_2O \rightarrow CH_4 + HCO_3^-. \quad (5)$$

Thus, although both reactions promote an increase in $\delta^{13}C$-DIC, acetate fermentation increases [DIC] whereas CO_2 reduction decreases [DIC]. The fact that the increase in $\delta^{13}C$-DIC of deep water in Georgetown Lake was accompanied by a sharp increase in [DIC] (Fig. 8) is evidence that reaction (5) was the dominant pathway for methanogenesis. Previous workers (Whiticar and Faber 1986; Whiticar et al. 1986) have shown that reaction (5) usually dominates over CO_2 reduction in freshwater sediments. A sample from the bottom of the water column collected at GT-2 in April 2013 returned a $\delta^{13}C$-CH_4 value of -0.7 ± 0.3 ‰. This value is within the range of $\delta^{13}C$ reported for methane formed from acetate fermentation in fresh water environments (Whiticar et al. 1986).

A typical value for the C-isotopic fractionation of CO_2 formed by reaction (5) in freshwater sediments is +20 ‰ (Stiller and Magaritz 1974; Gu et al. 2004). If we adopt this value and assume an average $\delta^{13}C$ of −25 ‰ for CO_2 derived from aerobic/anaerobic R (including CO_2 produced from BSR), then simple mass balance dictates that the rate of production of DIC by acetoclastic methanogenesis [reaction (5)] must have exceeded the rate of production of DIC by R for $\delta^{13}C$-DIC to increase. In addition, it is possible that other reactions, such as dissolution of carbonate minerals, could modify the DIC mass balance. As mentioned previously, SIs for calcite were negative at all depths throughout the winter months. Carbonate mineral dissolution is supported by the increase in $[Ca^{2+}]$ towards the bottom of the water column at GT-2 (Fig. 5e). Although $CaCO_3$ has been identified in shallow sediment from Georgetown Lake in the form of gastropod shells, no $\delta^{13}C$-$CaCO_3$ data are available at the time of this writing.

An interesting question that is presently unanswered deals with the fate of the CH_4 produced near the sediment–water interface in Georgetown Lake. Because of strong stratification under ice cover, much of the CH_4 remains dissolved in the lower portion of the water column until ice-off, at which time strong winds induce vertical mixing and promote evasion of CH_4 to the atmosphere. This scenario has been documented from other high-latitude lakes, and may be important in the global CH_4 budget (Michmerhuizen et al. 1996; Huttunen et al. 2003). It is also possible that some CH_4 may rise to the base of the ice as bubbles of CO_2–N_2–CH_4 gas mixtures (i.e., ebullition) which then may be frozen into the ice (Anthony et al. 2010; Boereboom et al. 2012). Oxidation and assimilation of CH_4 by methanotrophs is another potentially important sink (Bastviken et al. 2003; Lehmann et al. 2004; Utsumi et al. 1998).

Sulfur cycling under ice cover

The S-isotopic composition of sulfate in the shallow water column at GT-2 (9.7 ‰) is similar to the average S-isotopic composition of sulfate in the major tributaries to the lake (9.2 ‰; Table 4). Given the existence of H_2S in the deep water column, the $\delta^{34}S$ of sulfate might be expected to increase owing to BSR, which produces isotopically light H_2S. S-isotope fractionation accompanying BSR using natural organic matter as substrate varies from 30 to 40 ‰, as long as concentrations of sulfate are non-limiting (Canfield 2001). However, at low sulfate concentrations (<1 mM), S-isotope fractionation during BSR approaches zero (Harrison and

Thode 1958; Canfield and Raiswell 1999). Given the very low concentrations of sulfate in Georgetown Lake (<0.1 mM) coupled with the small observed S-isotope separation between H_2S and SO_4^{2-}, it can be assumed that BSR in the lake is strongly sulfate-limited. If all sulfate was reduced to sulfide, then $\delta^{34}S$ of sulfide would be the same as $\delta^{34}S$ of sulfate in the overlying water column. At GT-2, the average of three $\delta^{34}S$-sulfide values (6.7 ‰) was slightly lower than the $\delta^{34}S$ of sulfate in the upper water column (9.7 ‰; Table 4). This suggests that the majority of the sulfate was reduced to sulfide.

In contrast to $\delta^{34}S$, sulfate in the shallow water at GT-2 has a much lower value of $\delta^{18}O$ (−6.4 ‰) compared to sulfate in the major tributaries (2.8, 0.8 ‰; Table 4). This can be explained by internal cycling of S within the lake. In winter, much of the sulfate in the lake is reduced to H_2S by BSR. After ice-off and spring overturn, much of this H_2S is probably re-oxidized to sulfate. This reaction typically involves formation of SO_3^- as an intermediate species. Although the rate of O-isotope exchange between SO_4^{2-} and water is negligible at low temperature, a number of studies have shown that exchange of O-isotopes is rapid between SO_3^- and water (Lloyd 1968; Seal II 2003). Thus, SO_4^{2-} formed by oxidation of H_2S may derive a considerable fraction of its O atoms from water in the lake, which—in the case of Georgetown Lake—is isotopically light (average $\delta^{18}O$-H_2O at GT-2 = −14.7 ‰).

Conceptual site models

Using the cumulative data presented in this paper, we have developed conceptual models to explain vertical changes in water chemistry at both sampling locations (Fig. 10). Based on the concentrations and isotopic compositions of DO, oxygenic P under snow and ice cover was more important at the shallower GT-2 site compared to GT-1. One possible explanation for this difference is that the supply of nutrients to the photic zone at GT-1 is limited by deep currents which intercept solutes diffusing upward from the sediment, discharging them at the dam. In any event, [DO] remained sufficiently high to allow overwinter survival of salmonids at GT-2, although the fish were most likely confined to the top meter of the water column by winter's end. A second important difference between the two sampling sites was the presence of a purple-pigmented layer of putative S-oxidizing bacteria about 1–2 m above the bottom of the lake at GT-2, but not at GT-1. If the purple bacteria are anoxygenic H_2S-oxidizing phototrophs, the absence a purple layer at GT-1 could be related to the lower H_2S concentrations at this site, or to the fact that the euxinic zone at GT-1 is about 3 m deeper than at GT-2 and therefore may lie below the photic zone.

Some other differences between GT-1 and GT-2 can be linked to hydrology. As mentioned earlier, the outlet pipes at Georgetown Lake dam are located near the bottom of the water column, and consequently they discharge higher-salinity bottom water. This, combined with a steeper topographic gradient in the narrow outlet bay of the lake, would create a slow current of deep, dense water heading towards the outlet pipes (Fig. 10b). Solutes diffusing upwards from sediment at GT-1 would have become entrained into this current and thence advected away, rather than accumulating in the deep water column, as at GT-2. This may help to explain why increases in solute concentrations with depth as well as vertical changes in $\delta^{13}C$-DIC were less dramatic at GT-1 compared to GT-2. As well, water isotope profiles (Fig. 2) suggest mixing of lake water and upwelling groundwater at GT-1, but not at GT-2.

Conclusions

We have combined chemistry and stable isotopes to better understand biogeochemical processes taking place beneath ice cover in a shallow, highly productive lake over the course of a winter season. In the period of time between ice formation in November and ice-off in late May, [DO] decreased while [DIC] increased, consistent with rates of aerobic R exceeding rates of oxygenic P. Nonetheless, based on an interpretation of seasonal and vertical trends in [DO] and $\delta^{18}O$-DO, significant below-ice oxygenic P occurred, with higher P rates at a shallower monitoring site (GT-2) as compared to a deeper channel near the dam outlet (GT-1). At GT-2, oxygenic P allowed the top meter of the water column to remain sufficiently oxic to allow over-winter survival of fish. Water near the bottom of the lake at both sampling sites was anoxic, sulfidic, highly enriched in DIC and ammonium, and slightly enriched in dissolved Fe, Mn, SRP, and silica. These

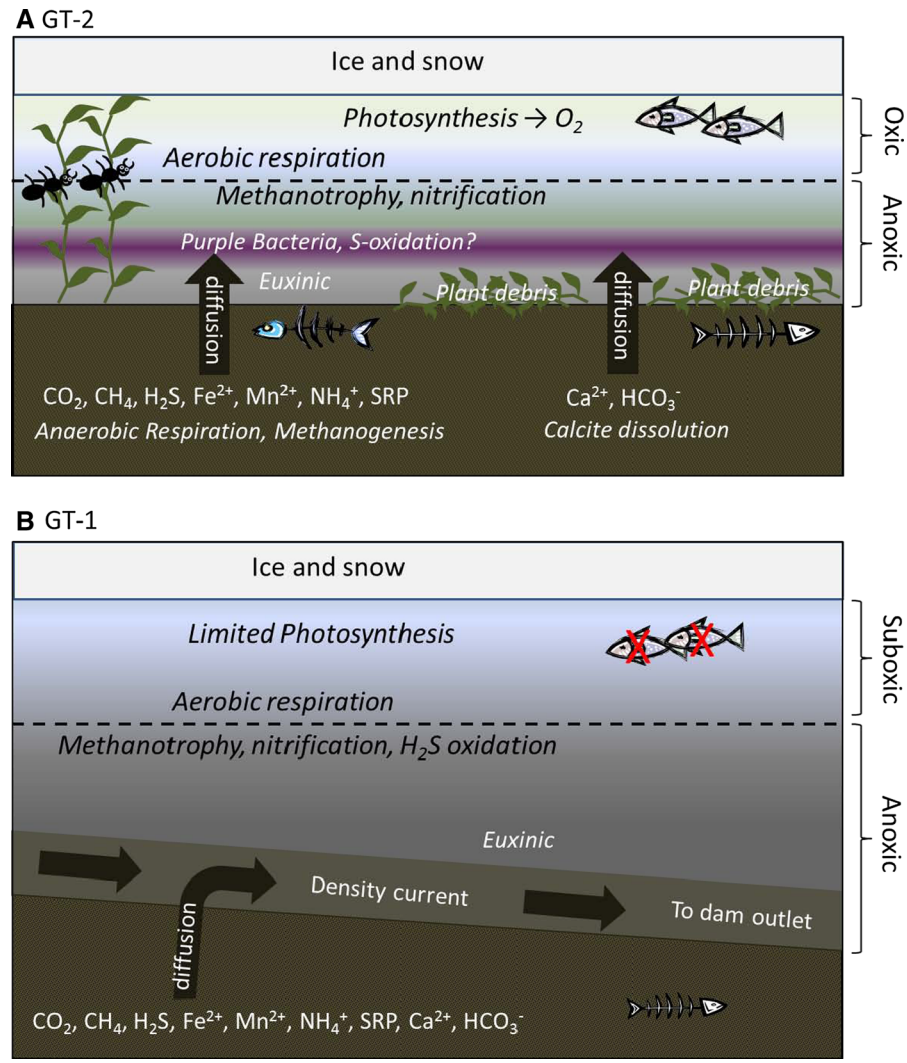

Fig. 10 Conceptual models summarizing hydrological, geochemical, and biological processes impacting water quality at GT-2 (*top*) and GT-1 (*bottom*). A lush growth of pondweed at GT-2 in early winter (*top left*) dies back to roots in winter, creating a large mass of biodegradable organic carbon at the bottom of the lake (*top right*)

trends, which were more pronounced at GT-2 as compared to GT-1, are explained by upward diffusion from sediment-pore water where organic matter was being decomposed.

Stable isotopes of DIC were particularly helpful in this study to track biogeochemical processes under ice cover in Georgetown Lake. Values of δ^{13}C-DIC initially decreased in response to net production of isotopically light CO_2 by R, but then showed a sharp increase in the deep water towards the end of the ice-covered season. This increase in δ^{13}C-DIC, accompanied by a sharp increase in [DIC] and [CH_4], is attributed to acetoclastic methanogenesis near the sediment–water interface, a process that produces ^{13}C-enriched DIC. Methanogenesis was likely favored by a lack of competition for organic substrates from sulfate reducing bacteria, whose activity was constrained by very low sulfate concentrations (Lovley and Klug 1983). Although some CH_4 may have been consumed within the water column by methanotrophs, an unquantified mass of methane likely escaped to the atmosphere during spring turnover, which occurred within 48 h of ice-off.

Seasonal temperature averages and extremes in western Montana have been increasing two–three times faster than the global average (Pederson et al. 2010); hence, decreases in the duration of seasonal ice cover may be particularly rapid among the lakes of this region. In Georgetown Lake, under-ice P was significant at shallow depth and possibly critical to over-

winter survival of fish. Nonetheless, Georgetown Lake was R-dominated in winter, becoming methanogenesis-dominated near the sediment–water interface. Stratification due to ice cover allowed for the development of steep vertical gradients in the concentrations of O_2, CO_2, CH_4, NH_4^+, NH_4^+, SO_4^{2-}, H_2S, Fe^{2+}, and Mn^{2+} at the sub-meter scale, creating a complex hierarchy of potential ecological niches for heterotrophic and photosynthetic (both oxygenic and anoxygenic) microbes. Ice cover-induced stratification clearly structures the biogeochemical environment; however, the consequences of a longer ice-free period for fisheries depend critically on the P–R balance, which may be sensitive to other factors such as temperature and organic carbon loading. Future studies will attempt to link the observed chemical and isotopic gradients at Georgetown Lake to spatial and temporal changes in carbon pools and specific microbial populations and rate processes.

Acknowledgments This research was partly funded by collaborative Grants 0739054 and 0738912, with follow-up support from NSF-EPSCoR and the Montana Institute on Ecosystems. We thank Craig Stafford (University of Montana) for sharing his ideas and data on Georgetown Lake. This paper was substantially improved by the comments of two anonymous reviewers and the Associate Editor, R. Kelman Wieder.

References

Allison JD, Brown DS, Novo-Gradac KJ (1991) MINTEQA2/PRODEFA2, a geochemical assessment model for environmental systems. US Environmental Protection Agency, EPA/600/3-91/021

Angert A, Luz B, Yakir D (2001) Fractionation of oxygen isotopes by respiration and diffusion in soils and its implications for the isotopic composition of atmospheric O_2. Glob Biogeochem Cycles 15:871–880

Anthony KM, Vas D, Brosius L, Chapin F III, Zimov SA, Zhuang Q (2010) Estimating methane emissions from northern lakes using ice-bubble surveys. Limnol Oceanogr Methods 8:592–609

Assayag N, Jézéquel D, Ader M, Viollier E, Michard G, Prévot F, Agrinier P (2008) Hydrological budget, carbon sources and biogeochemical processes in Lac Pavin (France): constraints from $\delta^{18}O$ of water and $\delta^{13}C$ of dissolved inorganic carbon. Appl Geochem 23:2800–2816

Babin J, Prepas EE (1985) Modelling winter oxygen depletion rates in ice-covered temperate zone lakes in Canada. Can J Fish Aquat Sci 42:239–249

Bade DL, Carpenter SR, Cole JJ, Hanson PC, Hesslein RH (2004) Controls of $\delta^{13}C$-DIC in lakes: geochemistry, lake metabolism, and morphometry. Limnol Oceanogr 49: 1160–1172

Bass AM, Waldron S, Preston T, Adams CE, Drummond J (2010a) Temporal and spatial heterogeneity in lacustrine $\delta^{13}C_{DIC}$ and $\delta^{18}O_{DO}$ signatures in a large mid-latitude temperate lake. J Limnol 69:341–349

Bass AM, Waldron S, Preston T, Adams CE (2010b) Net pelagic heterotrophy in mesotrophic and oligotrophic basins of a large, temperate lake. Hydrobiologia 652:363–375

Bastviken D, Ejlertsson J, Sundh I, Tranvik L (2003) Methane as a source of carbon and energy for a lake pelagic food web. Ecology 84:969–981

Bastviken DJ, Cole J, Pace M, Tranvik L (2004) Methane emissions from lakes: dependence of lake characteristics, two regional assessments, and a global estimate. Glob Biogeochem Cycles 18:GB4009

Benson BB, Krause D Jr (1980) The concentration and isotopic fractionation of gases dissolved in freshwater in equilibrium with the atmosphere: 1, oxygen. Limnol Oceanogr 25:662–671

Bertilsson S, Burgin A, Carey CC, Fey SB, Grossart H-P, Grubisic LM, Jones ID, Kirillin G, Lennon JT, Shade A, Smyth RL (2013) The under-ice microbiome of seasonally frozen lakes. Limnol Oceanogr 58:1998–2012

Boereboom T, Depoorter M, Coppens S, Tison JL (2012) Gas properties of winter lake ice in Northern Sweden: implication for carbon gas release. Biogeosciences 9:827–838

Brandes JA, Devol AH (1997) Isotopic fractionation of oxygen and nitrogen in coastal marine sediments. Geochim Cosmochim Acta 61:1793–1801

Brown JM, Poulson SR (2010) Biogeochemical controls on seasonal variations of the stable isotopes of dissolved oxygen and dissolved inorganic carbon in Castle Lake, CA. In: AGU, fall meeting 2010, abstract #H54B-02

Canfield DE (2001) Isotope fractionation by natural populations of sulfate-reducing bacteria. Geochim Cosmochim Acta 65:1117–1124

Canfield DE, Raiswell R (1999) The evolution of the sulfur cycle. Am J Sci 299:697–723

Carmody RW, Plummer LN, Busenberg E, Coplen TB (1998) Methods for collection of dissolved sulfate and sulfide and analysis of their sulfur isotopic composition. US Geological Survey, Open File Report 997-234

Clark J, Fritz P (1997) Environmental isotopes in hydrogeology. Lewis Publishers, Boca-Raton

Craig H (1961) Isotopic variations in meteoric waters. Science 133:1702–1703

Dibike Y, Prowse T, Bonsal B, de Rham L, Saloranta T (2012) Simulation of North American lake-ice cover characteristics under contemporary and future climate conditions. Int J Climatol 32:695–709

Dunnette DA, Chynoweth DP, Khalil HM (1985) The source of hydrogen sulfide in anoxic sediment. Water Res 19:875–884

Epstein S, Mayeda T (1953) Variation of O-18 content of waters from natural sources. Geochim Cosmochim Acta 4: 213–224

Falkowski PG, Raven JA (1997) Aquatic photosynthesis. Blackwell Sciences, Oxford

Gammons CH, Poulson SR, Pellicori DA, Roesler A, Reed PJ, Petrescu EM (2006) The hydrogen and oxygen isotopic composition of precipitation, evaporated mine water, and river water in Montana, USA. J Hydrol 328:319–330

Gammons CH, Pape BL, Parker SR, Poulson SR, Blank CE (2013) Geochemistry, water balance, and stable isotopes of a "clean" pit lake at an abandoned tungsten mine, Montana, USA. Appl Geochem 36:57–69

Garrett PA (1983) Relationships between benthic communities, land use, chemical dynamics, and trophic state in Georgetown Lake. PhD Dissertation, Montana State University

Garrison RJ (1976) Sediment chemistry of Georgetown Lake, Montana. MS Thesis, Montana State University

Gibson JAE (1999) The meromictic lakes and stratified marine basins of the Vestfold Hills, East Antarctica. Antarct Sci 11:175–192

Giesemann A, Jager HJ, Norman AL, Krouse HP, Brand WA (1994) On-line sulfur-isotope determination using an elemental analyzer coupled to a mass spectrometer. Anal Chem 66:2816–2819

Greenbank J (1945) Limnological conditions in ice-covered lakes, especially as related to winterkill of fish. Ecol Monogr 15:343–392

Gu B, Schelske CL, Hodell DA (2004) Extreme ^{13}C enrichments in a shallow hypereutrophic lake: implications for carbon cycling. Limnol Oceanogr 49:1152–1159

Guy RD, Fogel ML, Berry JA (1993) Photosynthetic fractionation of the stable isotopes of oxygen and carbon. Plant Physiol 101:37–47

Harris D, Porter LK, Paul EA (1997) Continuous flow isotope ratio mass spectrometry of carbon dioxide trapped as strontium carbonate. Commun Soil Sci Plant Anal 28:747–757

Harrison AG, Thode HG (1958) Mechanisms of the bacterial reduction of sulfate from isotope fractionation studies. Trans Faraday Soc 53:84–92

Herczeg AL (1987) A stable carbon isotope study of dissolved inorganic carbon cycling in a softwater lake. Biogeochemistry 4:231–263

Huttunen JT, Alm J, Lukanen A, Juutinen S, Larmola T, Hammar T, Silvola J, Martikainen PJ (2003) Fluxes of methane, carbon dioxide and nitrous oxide in boreal lakes and potential anthropogenic effects on the aquatic greenhouse gas emissions. Chemosphere 52:609–621

Karim A, Dubois K, Veizer J (2011) Carbon and oxygen dynamics in the Laurentian Great Lakes: implications for the CO_2 flux from terrestrial aquatic systems to the atmosphere. Chem Geol 281:133–141

Kiddon J, Bender ML, Orchardo J, Caron DA, Goldman JC, Dennett M (1993) Isotope fractionation of oxygen by respiring marine organisms. Glob Biogeochem Cycles 7:679–694

Knight JC (1981) An investigation of the general limnology of Georgetown Lake, Montana. PhD Dissertation, Montana State University

Kornexl BE, Gehre M, Höffling R, Werner RA (1999) On-line $\delta^{18}O$ measurement of organic and inorganic substances. Rapid Commun Mass Spectrom 13:1685–1693

Kroopnick PM (1975) Respiration, photosynthesis and oxygen isotope fractionation in oceanic surface water. Limnol Oceanogr 20:988–992

Kurz WA, Dymond CC, Stinson G, Rampley GJ, Neilson ET, Carroll AL, Ebata T, Safranyik L (2008) Mountain pine beetle and forest carbon feedback to climate change. Nature 452:987–990

Lane GA, Dole M (1956) Fractionation of oxygen isotopes during respiration. Science 123:574–576

Lehmann MF, Bernasconi SM, McKenzie JA, Barbieri A, Simona M, Veronesi M (2004) Seasonal variation of the $\delta^{13}C$ and $\delta^{15}N$ of particulate and dissolved carbon and nitrogen in Lake Lugano: constraints on biogeochemical cycling in a eutrophic lake. Limnol Oceanogr 49:415–429

Lloyd RM (1968) Oxygen isotope behavior in the sulfate–water system. J Geophys Res 73:6099–6110

Lonn JD, McDonald C, Lewis RS, Kalakay TJ, O'Neill JM, Berg RB, Hargrave P (2003) Preliminary geologic map of the Philipsburg $30' \times 60'$ quadrangle, western Montana. Montana Bureau of Mines and Geology, Open File 483

Lovley DR, Klug MJ (1983) Sulfate reducers can outcompete methanogens at freshwater sulfate concentrations. Appl Environ Microbiol 45:187–192

Luz B, Barkan E, Sagi Y, Yacobi YZ (2002) Evaluation of community respiratory mechanisms with oxygen isotopes: a case study in Lake Kinneret. Limnol Oceanogr 47:33–42

Mandernack KW, Mills CT, Johnson CA, Rahn T, Kinney C (2009) The $\delta^{15}N$ and $\delta^{18}O$ values of N_2O produced during the co-oxidation of ammonia by methanotrophic bacteria. Chem Geol 267:96–107

Mathias JA, Barica J (1980) Factors controlling oxygen depletion in ice-covered lakes. Can J Fish Aquat Sci 37:185–194

Michmerhuizen CM, Striegl RG, McDonald ME (1996) Potential methane emission from north-temperate lakes following ice melt. Limnol Oceanogr 41:985–991

Morrison J, Brockwell T, Merren T, Fourel F, Phillips AM (2001) On-line high precision stable hydrogen isotopic analyses on nanoliter water samples. Anal Chem 73: 3570–3575

Myrbo A, Shapley MD (2006) Seasonal water-column dynamics of dissolved inorganic carbon stable isotope compositions ($\delta^{13}C_{DIC}$) in small hardwater lakes in Minnesota and Montana. Geochim Cosmochim Acta 70:2699–2714

Oba Y, Poulson SR (2009a) Oxygen isotope fractionation of dissolved oxygen during abiological reduction by aqueous sulfide. Chem Geol 268:226–232

Oba Y, Poulson SR (2009b) Oxygen isotope fractionation of dissolved oxygen during reduction by ferrous iron. Geochim Cosmochim Acta 73:13–24

Parker SR, Poulson SR, Gammons CH, DeGrandpre M (2005) Biogeochemical controls on diel cycles in the stable isotopic composition of dissolved O_2 and DIC in the Big Hole River, Montana, USA. Environ Sci Technol 39:7134–7140

Parker SR, Gammons CH, Poulson SR, DeGrandpre MD, Weyer CL, Smith MG, Babcock JN, Oba Y (2010) Diel behavior of stable isotopes of dissolved oxygen and dissolved inorganic carbon in rivers over a range of trophic conditions, and in a mesocosm experiment. Chem Geol 269:22–32

Parker SR, Darvis MN, Poulson SR, Gammons CH, Stanford JA (2014) Dissolved oxygen and dissolved inorganic carbon stable isotope composition and concentrations fluxes across several shallow floodplain aquifers and in a diffusion experiment. Biogeochemistry 117:539–552

Pederson GT, Graumlich LJ, Fagre DB, Kipfer T, Muhlfeld CC (2010) A century of climate and ecosystem change in western Montana: what do temperature trends portend? Clim Change 98:133–154

Poulson SR, Sullivan AB (2010) Assessment of diel chemical and isotopic techniques to investigate biogeochemical cycles in the upper Klamath River, Oregon, USA. Chem Geol 269:3–11

Quay PD, Emerson SR, Quay BM, Devol AH (1986) The carbon cycle for Lake Washington—a stable isotope study. Limnol Oceanogr 31:596–611

Quay PD, Wilbur DO, Richey JE, Devol AH (1995) The ^{18}O:^{16}O of dissolved oxygen in rivers and lakes of the Amazon Basin: determining the ratio of respiration to photosynthesis rates in freshwaters. Limnol Oceanogr 40:718–729

Raleigh RF, Hickman T, Soloman RC, Nelson PC (1984) Habitat suitability information: rainbow trout (*Oncorhynchus mykiss*). US Fish Wildlife Service: FWS/OBS-82/10.60

Scidmore WJ (1957) An investigation of carbon dioxide, ammonia, and hydrogen sulfide as factors contributing to fish kills in ice-covered lakes. Progress Fish Cult 19:124–127

Seal RR II (2003) Stable-isotope geochemistry of mine waters and related solids. In: JL Jambor, DW Blowes, AIM Ritchie, eds. Environmental Aspects of Mine Wastes. Miner Soc Can Short Course Ser 31:303–334

Shaw GE, White ES, Gammons CH (2013) Characterizing groundwater–lake interaction and its impact on lake water quality. J Hydrol 492:69–78

Smith MG, Parker SR, Gammons CH, Poulson SR, Hauer FR (2011) Tracing dissolved O_2 and dissolved inorganic carbon stable isotope dynamics in the Nyack aquifer: Middle Fork Flathead River, Montana, USA. Geochim Cosmochim Acta 75:5971–5986

Stafford CP (2013) Long-term trends in the water quality of Georgetown Lake, Montana. Prepared for Montana Department of Justice and Montana Department of Environmental Quality

Stiller M, Magaritz M (1974) Carbon-13 enriched carbonate in interstitial waters of Lake Kinneret sediments. Limnol Oceanogr 19:849–853

Trabert MJ (1993) The depletion of oxygen in Georgetown Lake, Montana, during the winter months. MS Thesis, Montana Tech

Tranvik LJ et al. (2009) Lakes and reservoirs as regulators of carbon cycling and climate. Limnol Oceanogr 54: 2298–2314

US Environmental Protection Agency (1976) Preliminary report on Georgetown Lake, national eutrophication survey. CERL, Corvallis

Usdowski E, Hoefs J, Menschel G (1979) Relationship between ^{13}C and ^{18}O fractionation and changes in major element composition in a recent calcite-depositing spring—a model of chemical variations with inorganic $CaCO_3$ precipitation. Earth Planet Sci Lett 42:267–276

Utsumi M, Nojiri Y, Nakamura T, Nozawa T, Otsuki A, Seki H (1998) Oxidation of dissolved methane in a eutrophic, shallow lake: Lake Kasumigaura, Japan. Limnol Oceanogr 43:471–480

Wachniew P, Rozanski K (1997) Carbon budget of a mid-latitude, groundwater-controlled lake: isotopic evidence for the importance of dissolved inorganic carbon recycling. Geochim Cosmochim Acta 61:2453–2465

Wang X, Veizer J (2000) Respiration–photosynthesis balance of terrestrial aquatic ecosystems, Ottawa area, Canada. Geochim Cosmochim Acta 64:3775–3786

Wang X, Depew D, Schiff S, Smith REH (2008) Photosynthesis, respiration, and stable isotopes of oxygen in a large oligotrophic lake (Lake Erie, USA-Canada). Can J Fish Aquat Sci 65:2320–2331

Wassenaar LI, Koehler G (1999) An on-line technique for the determination of the delta O-18 and delta O-17 of gaseous and dissolved oxygen. Anal Chem 71:4965–4968

Weyhenmeyer GA, Livingstone DM, Meili M, Jensen O, Benson B, Magnuson JJ (2011) Large geographical differences in the sensitivity of ice-covered lakes and rivers in the Northern Hemisphere to temperature changes. Glob Change Biol 17:268–275

Whiticar MJ (1999) Carbon and hydrogen isotope systematics of bacterial formation and oxidation of methane. Chem Geol 161:291–314

Whiticar MJ, Faber E (1986) Methane oxidation in sediment and water column environments—isotope evidence. Org Geochem 10:759–768

Whiticar MJ, Faber E, Schoell M (1986) Biogenic methane formation in marine and freshwater environments: CO_2 reduction vs. acetate fermentation—isotope evidence. Geochim Cosmochim Acta 50:693–709

Wiesenburg DA, Guinasso NL Jr (1979) Equilibrium solubilities of methane, carbon monoxide and hydrogen in water and sea water. J Chem Eng Data 24:356–360